

Thermo-optical and magneto-optical characteristics of CeF₃ crystal



Evgeniy A. Mironov^{a,*}, Aleksey V. Starobor^a, Ilya L. Snetkov^a, Oleg V. Palashov^a, Hiroaki Furuse^b, Shigeki Tokita^c, Ryo Yasuhara^d

^a Institute of Applied Physics of the Russian Academy of Sciences, 46 Ul'yanov Street, Nizhny Novgorod, 603950, Russia

^b Kitami Institute of Technology, 165 Koen-cho, Kitami, Hokkaido, 090-8507, Japan

^c Institute of Laser Engineering, Osaka University, 2-6 Yamada-oka, Suita, Osaka, 565-0871, Japan

^d National Institute for Fusion Science, 322-6, Oroshi-cho, Tokyo, Gifu, 509-5292, Japan

ARTICLE INFO

Article history:

Received 3 February 2017

Received in revised form

28 March 2017

Accepted 14 April 2017

Available online 24 April 2017

Keywords:

Magneto-active materials

Thermal effects

Birefringence

Depolarization

ABSTRACT

Thermo-optical and magneto-optical characteristics of a uniaxial CeF₃ crystal have been investigated. Its optical anisotropy parameter, magneto-optical figure of merit, and the ratio of the thermo-optical constants *P* and *Q* have been measured. The found characteristics have been compared with the corresponding values for the TGG crystal. Based on the obtained results it has been concluded that, despite its anisotropy, the CeF₃ crystal is promising material for the development of Faraday isolators for high-power lasers.

© 2017 Elsevier B.V. All rights reserved.

1. Introduction

A permanent increase of the average power of pulse-periodic and cw lasers makes improvement of different optical elements increasingly more important. Suppression of the thermally induced effects caused by radiation absorption becomes the main requirement to be met. One of the key elements of the majority of laser systems is the optical isolator – the Faraday isolator (FI) that is also sensitive to thermal self-action due to a relatively high absorption in the magneto-optical elements (MOE). The temperature distribution nonuniform over the MOE cross-section results, in particular, in appearance of phase distortions (thermal lens) and mechanical stresses giving rise to linear birefringence (photo-elastic effect). The isolation ratio is the most important FI characteristic. It is determined mainly by thermally induced depolarization caused by the photo-elastic effect; therefore the isolation ratio deteriorates with increasing radiation power. It is one of the most important basic problems in high-power laser engineering. One of the ways towards its solution is a search for magneto-active media

with good thermo-optical properties.

The most popular medium used as MOE in optical isolators for high-power lasers nowadays is a terbium-gallium garnet (TGG) crystal. However, thanks to the advances in production technologies of new optical crystals and ceramics a number of optical media with better thermal and magneto-optical properties are already known, for example, TSAG [1–3] and NTF [4] crystals, as well as TAG [5] and Ce:TAG [6] ceramics.

Absolute majority of FIs are based on optically isotropic media, such as cubic crystals, glasses, and ceramics as they are easy to work with and the devices based on them are easier to adjust. However, optical isolators can also be realized using of anisotropic media [7]. Some of anisotropic magneto-active crystals are attractive thanks to their unique characteristics. One of such media is an uniaxial CeF₃ crystal. The value of the Verdet constant for this crystal is close to that of the TGG crystal, but CeF₃ has a lower absorption coefficient and a wider transmission band [8,9].

A significant advantage of this crystal over other new experimental magneto-active media is a proven production technology so far as this material has long been used in scintillation detectors [10,11]. Another important advantage from the viewpoint of using this material in high-power laser systems is a possibility of producing from CeF₃ large-aperture (up to ~10 cm) optical elements. In this respect CeF₃ surpasses most of the magneto-active crystal media. For example, the largest aperture of a TGG single crystal

* Corresponding author.

E-mail addresses: miea209@rambler.ru (E.A. Mironov), astarobor@mail.ru (A.V. Starobor), snetkov@appl.sci-nnov.ru (I.L. Snetkov), palashov@appl.sci-nnov.ru (O.V. Palashov), furuse@mail.kitami-it.ac.jp (H. Furuse), tokita-s@ile.osaka-u.ac.jp (S. Tokita), yasuhara@nifs.ac.jp (R. Yasuhara).

with quality fit for producing an FI is 40 mm [12].

These features make the CeF_3 crystal attractive for using it in FIs for high-power lasers. Therefore, its thermo-optical characteristics need to be studied for assessing a possibility of using it in the field of high-power laser engineering.

All investigations were carried out for optical elements cut along the optical axis because only in this case the intrinsic birefringence can be excluded from consideration and Faraday isolator can be realized. Therefore all the presented results of the investigation of thermo-optical and magneto-optical characteristics are suitable only for this crystal orientation.

2. Magneto-optical properties

We chose for our studies a 7.5 mm long CeF_3 crystal with a diameter of 10 mm (Fig. 1) produced by Kinheng Crystal Material Ltd. We measured the dependence of the Verdet constant on wavelength at room temperature in the 450–1550 nm range by using lasers which have eight different wavelengths (405 nm, 450 nm, 532 nm, 633 nm, 810 nm, 980 nm, 1075 nm, 1310 nm, 1550 nm). The dispersion dependence of Verdet constant had also been measured in the earlier works [8,9], but not for the wavelengths over 800 nm, whereas the majority of the available high-power lasers operate in this range.

The studied sample was placed in a permanent-magnet magnetic system with known field distribution. The maximum value of the system's field was 2.45 T. The value of the Verdet constant was determined by the measured angle of rotation of the polarization plane from the known field distribution and crystal location in it. The measurements were made by the extinction method [13]. Laser diodes with output power of 10–20 mW were used as sources of radiation. Such power level was enough to provide high contrast during measurements that do not affect on measurement error.

The results of those experiments are presented in Table 1 and are shown in graph in Fig. 2. Accuracy of measurements of the angle of rotation of the polarization plane was limited by optical quality of used sample and was not worse than 2% throughout all spectral range. The magnetic field was measured by a Mayak-5 teslameter (Saratov, Russia) with a relative uncertainty within 1%. Thus, the measurement error of the Verdet constant did not exceed 3%.

The measured values were used to find the dependence of the Verdet constant of the CeF_3 crystal on the radiation wavelength $V(\lambda)$. In the approximation based on the assumption that the rotation of the plane of polarization is determined only by one transition, the $V(\lambda)$ dependence is represented in the form

$$V = \frac{A}{\lambda^2 - \lambda_0^2} \quad (1)$$

This dependence was used for approximation of the experimental data. The parameters A and λ_0 were found by the least squares method to be $\lambda_0 = 246$ nm and $A = 4.1 \cdot 10^7$ rad \cdot nm 2 /(T \cdot m), which coincides to a good accuracy with the analogous values

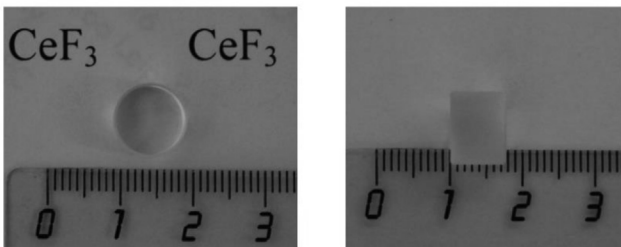


Fig. 1. Photographs of CeF_3 single crystal.

Table 1
Magneto-optical properties of CeF_3 and TGG crystals.

λ , nm	$V(\lambda)$, rad/(T m)								
	405	450	532	633	810	980	1075	1310	1550
CeF_3		300.5	191.8	124.5	68.6	45	36.6	21.7	13.8
TGG	466.5		209.1	135.8	75.9		37	20.7	8.9

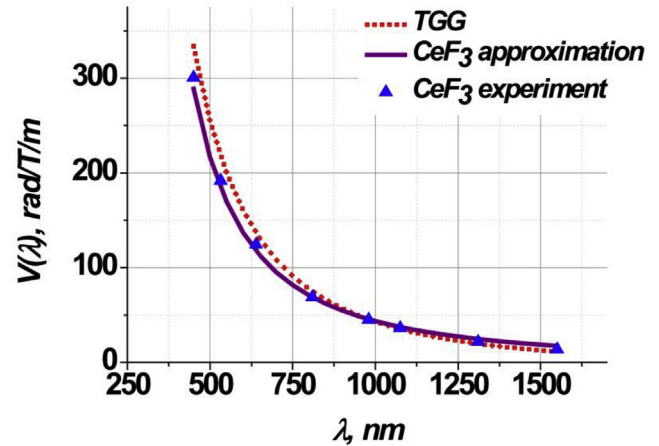


Fig. 2. Experimentally measured dispersion of the Verdet constant of CeF_3 crystal (triangles), approximation of this dispersion (solid line) and the dispersion of the Verdet constant of TGG crystal (dashed line).

calculated in Ref. [8]. The obtained $V(\lambda)$ dependence is plotted in Fig. 2 from which it is clear that the experimental results are well approximated by it throughout the studied wavelength range. Deviations of experimental data from this dependence do not exceed 3% measurement error.

The curve for the Verdet constant of the TGG crystal measured in Ref. [2] is shown for comparison in Table 1 and in Fig. 2. It is clear that the Verdet constants of TGG and CeF_3 crystals almost coincide at the wavelength of 1075 nm (the difference is less than measurement error). At shorter wavelengths, this characteristic is higher for TGG, and the CeF_3 crystal has a larger Verdet constant in a longer wavelength region. This is explained by the fact that $V(\lambda)$ for the TGG crystal is not so well approximated by the dependence of the form (1) at the wavelength is more than 1 μm [2].

Besides, the CeF_3 crystal is transparent for radiation at the wavelengths up to 2 μm [9], whereas the TGG crystal becomes optically nontransparent starting from ~ 1.4 μm [14]. According to formula (1) and the measured values of λ_0 and A , the value of the Verdet constant for the radiation at the wavelength of 2 μm is about 8 ± 2 rad/(T \cdot m). Precision of this estimation is not high, because this wavelength is far from investigated range and the uncertainty of parameters A and λ_0 lead to high variation of the extrapolated value. Moreover the estimation may differ from actual value because the single transition model may be not very precise for longer wavelengths, therefore further experimental investigation of CeF_3 magneto-optical properties in this spectral range is needed. Nevertheless we can conclude that the CeF_3 crystal is promising for the development of FIs for powerful lasers with the wavelength of ~ 2 μm , which are currently of great interest for a wide scope of research.

3. Investigation of thermally induced depolarization

There is an ambiguity in the literature on crystallography as to

what class of symmetry the CeF_3 crystal belongs. In a number of papers it is stated that it is a crystal of trigonal system of $\bar{3}m$ symmetry group [15,16], the authors of some other works insist that it belongs to the hexagonal crystal system of $6/m\bar{m}$ symmetry group [17,18]. The symmetry group of the crystal, in particular, determines the form of the piezo-optical tensor π and of the elastic compliance tensor \mathbf{s} which specify the structure and magnitude of laser radiation polarization distortions arising as a result of its thermal action on the optical element. In our case, however, this ambiguity does not lead to the differences in the description of thermally induced effects.

The elastic compliance tensor and the piezo-optical tensor of trigonal and hexagonal crystals meet the following relations between their components [19]:

$$s_{66} = \frac{1}{2}(s_{11} - s_{12}) \quad (2)$$

$$\pi_{66} = \pi_{11} - \pi_{12}, \quad (3)$$

where s_{ij} and π_{ij} are the components of the elastic compliance tensor and of the piezo-optical tensor in the two-index notation.

The same relations for these tensor components \mathbf{s} and π are typical for media with isotropic elastic and piezo-optical properties, for example, glasses. These relations indicate that the elastic and piezo-optical properties of trigonal and hexagonal crystals are isotropic in the plane perpendicular to the optical axis. Thus, the thermally induced distortions in these crystals cut along the optical axis may be described by the same formulas as in isotropic media. The expression for the degree of depolarization γ defined as the ratio of the power of the depolarization radiation component P_d to its total power P_0 :

$$\gamma = \frac{P_d}{P_0} \quad (4)$$

for the case when the optical element is a cylinder with length L much greater than radius R_0 may be written as in Ref. [20]:

$$\gamma = \frac{A}{8} \left(\frac{L}{\lambda} \frac{\alpha Q}{\kappa} P_0 \right)^2, \quad (5)$$

where α is the absorption coefficient and A is the numerical coefficient determined by the laser beam profile and equal to 0.137 for the Gaussian intensity distribution [21]. Please note the difference from the isotropic case. First, here κ is understood as thermal conductivity in the direction perpendicular to the optical axis. Second, the quantity Q called a thermo-optical constant is defined by the expression different from that of the isotropic case. In particular, it is defined by the elastic stresses arising in the optical element under the action of heating radiation. The expressions for stresses in trigonal and hexagonal crystals differ from the isotropic case only by the factor determined by the components of the elastic compliance and thermal expansion tensors [22]. Thus, the expression for Q for the case of trigonal and hexagonal crystals cut along the optical axis may be written in the form

$$Q = \frac{n_0^3}{4} \frac{\alpha_{11}^T s_{33} - \alpha_{33}^T s_{13}}{s_{11} s_{33} - s_{13}^2} (\pi_{11} - \pi_{12}) \quad (6)$$

where n_0 in the unperturbed index of refraction and α_{ij}^T are the components of the thermal expansion tensor. In the isotropic case described by a smaller number of independent nonzero components of the elastic compliance and thermal expansion tensors

$$s_{11} = s_{33} = \frac{1}{E}; s_{13} = -\frac{\nu}{E} \quad (7)$$

$$\alpha_{11}^T = \alpha_{33}^T = \alpha^T \quad (8)$$

the expression (6) takes on the known form

$$Q = \frac{n_0^3}{4} \frac{\alpha^T E}{1 - \nu} (\pi_{11} - \pi_{12}) \quad (9)$$

where E is the Young's modulus and ν is the Poisson's ratio.

The isotropy of the piezo-optical properties of hexagonal and trigonal crystals cut along the optical axis expresses, in particular, in absence of dependence of the depolarization degree γ on the angle θ between the polarization plane and the crystallographic axis lying in the cross-section of the element (see Fig. 3). In the case of anisotropic piezo-optical properties, such dependence arises, for instance, in cubic crystals [24] and in tetragonal crystals cut along the optical axis [25]. It may be characterized by a special material constant – optical anisotropy parameter ξ that may be expressed through the components of the piezo-optic tensor

$$\xi = \frac{\pi_{66}}{\pi_{11} - \pi_{12}} \quad (10)$$

In our case, like in glasses, the equality (3) is fulfilled; therefore $\xi = 1$ and the polarization distortions do not depend on angle θ . The pattern of distribution of depolarized component of radiation in this case is a Maltese cross whose orientation is determined only by the position of the polarization plane and does not change when the element is rotated around its axis. In cubic and tetragonal crystals, the Maltese cross may oscillate or rotate [24,25].

For measuring thermo-optical characteristic of the CeF_3 crystal we performed a series of experiments on determining thermally induced depolarization in the studied sample. Although the shape of element was not rod (length L is 7.5 mm and the radius R_0 is 5 mm), obtained results could be described by formula (5) derived for this geometry. This approximation can be used because the diameter of the laser beam was ~ 1 mm that is much smaller than the length of element, so the distribution of thermal stresses causing photo-elastic effect was similar to the case of a rod.

The thermally induced depolarization was measured using the standard scheme with crossed polarizers [1,24]. The Yb-fiber laser ($\lambda = 1075$ nm) with maximum output power of 1.5 kW was used as a source of heating and probe radiation simultaneously.

First, we studied the behavior of the radiation depolarization component as a function of the relative position of the polarization

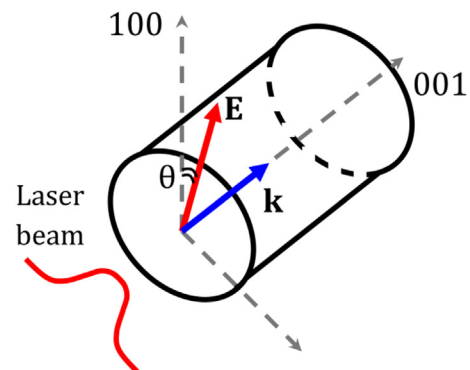


Fig. 3. Propagation of laser radiation with linear polarization \mathbf{E} through the optical element. The direction \mathbf{k} of radiation propagation coincides with the optical axis.

plane and the crystallographic axes. The CeF₃ sample was rotated around its axis when the radiation with a power of 850 W was transmitted through it. The distribution patterns of depolarized radiation are shown in Fig. 4 for several values of angle θ . As was expected, the Maltese cross did not change its orientation. Only intensity fluctuations were observed due to nonideal optical quality of the crystal. Thereby, it was confirmed experimentally that the optical anisotropy parameter of the CeF₃ crystal is equal to 1.

The dependence of the degree of the integral thermally induced depolarization on the power of the radiation passing through the sample was also measured. The results of those measurements are presented in Fig. 5.

It is clear from the plot that the so-called “cold” depolarization of the radiation passing through the sample is rather large. This is explained by a low optical quality of the crystal. That is why the radiation depolarization is almost power independent up to ~200 W. However, when the radiation power approaches 1 kW, this dependence becomes quadratic. From these data $\alpha|Q|/\kappa$ may be found as a fitting parameter that corresponds to the analogous parameter for the TGG crystal with absorption coefficient $\alpha = 1.5 \cdot 10^{-3} \text{ cm}^{-1}$ and is equal to $5.7 \times 10^{-8} \text{ W}^{-1}$. The power dependence of the depolarization degree in such a TGG crystal having the same length as the studied sample (7.5 mm) is plotted in Fig. 5. The parameter $\alpha|Q|/\kappa$ was found from the quadratic-dependent part of parabolic approximation of experimental dependence of depolarization degree on laser power. Accuracy of the determination of this parameter depends on number of experimental values and their scattering. It was about 7% in this particular case.

As the Verdet constant measurements have been presented in Sec.2, we can now determine the magnitude of the magneto-optical figure of merit of the studied crystal that is the most important characteristic of the magneto-optical medium [20]:

$$\mu = \frac{V\kappa}{Q\alpha} \quad (11)$$

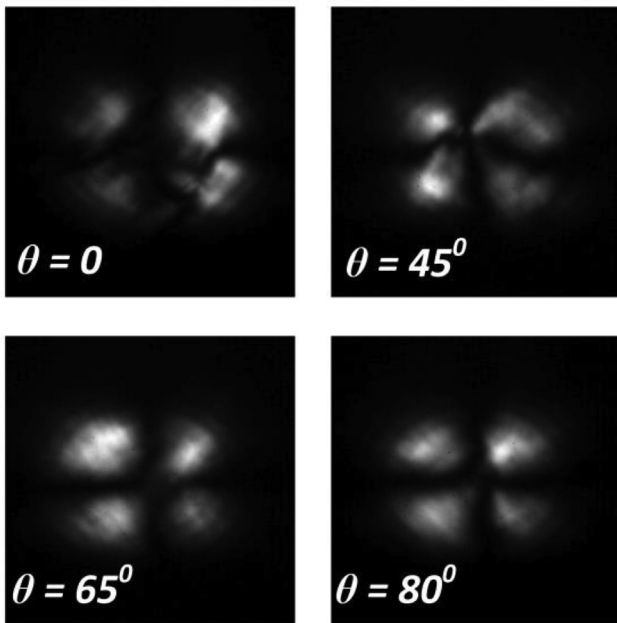


Fig. 4. Radiation depolarization component distribution in CeF₃ sample at power $P_0 = 850 \text{ W}$ for different values of the angle θ between the polarization plane and the crystallographic axis lying in the optical element cross-section.

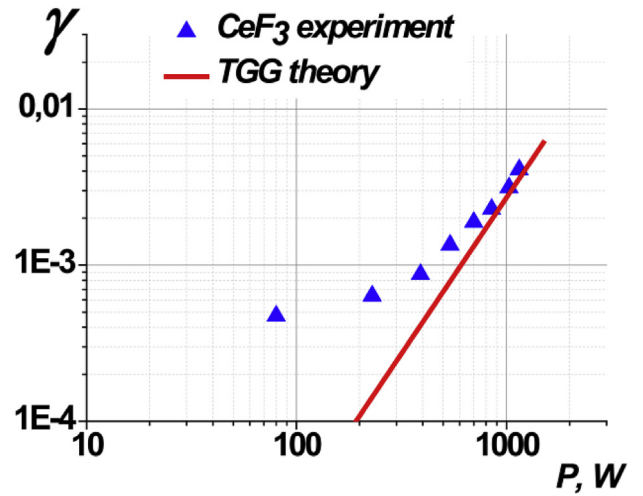


Fig. 5. Results of measurements of depolarization degree of the radiation passing through the studied CeF₃ sample as a function of its power (triangles) and analogous theoretical dependence for the TGG crystal sample with the same length and absorption coefficient $\alpha = 1.5 \cdot 10^{-3} \text{ cm}^{-1}$ (straight line).

This characteristic determines the magnitude of thermally induced depolarization in the FI at high-power radiation. After the substitution of the corresponding values, we obtain the value of the magneto-optical figure of merit of the CeF₃ crystal at the wavelength of 1075 nm: $\mu_{\text{CeF}_3} = 6.5 \times 10^8 \text{ rad W}^{-1}/(\text{T m})$. It corresponds to the magneto-optical figure of merit of a high-quality TGG crystal.

4. Thermal lens measurement

We assume that the magnitude of thermal lens in an optical element is determined only by changes in the index of refraction caused by its dependence on temperature and photo-elastic effect (variations of the element geometry as a result of heating are neglected). The changes in the index of refraction caused by the photo-elastic effect in hexagonal and trigonal crystals cut along the optical axis are not qualitatively different from the corresponding changes in media with isotropic elastic and piezo-optical properties (glasses, for example). As a consequence, the depolarization radiation component has an analogous qualitative behavior. A similar situation is typical for thermal lens.

For a Gaussian beam, the focal length F of the thermal lens in isotropic media is defined by Ref. [26]:

$$\frac{1}{F} = \frac{1}{4\pi a^2} \frac{\alpha L P}{\kappa} P_0, \quad (12)$$

where a is the beam radius, and P is another thermo-optical constant of the medium characterizing the wave aberration averaged over two orthogonal polarizations. For the isotropic media, the expression for P has the form [23,24]:

$$P = \left(\frac{dn}{dT} \right)_\sigma + \frac{n_0^3}{4} \frac{\alpha^T E}{1-\nu} (\pi_{11} + 3\pi_{12}), \quad (13)$$

where $\left(\frac{dn}{dT} \right)_\sigma$ is a derivative of index of refraction with respect to the temperature T for zero stresses.

The changes in the index of refraction caused by the photo-elastic effect in hexagonal and trigonal crystals are qualitatively described by the same formulas as in media with isotropic elastic and piezo-optical properties; therefore, part of the wave front

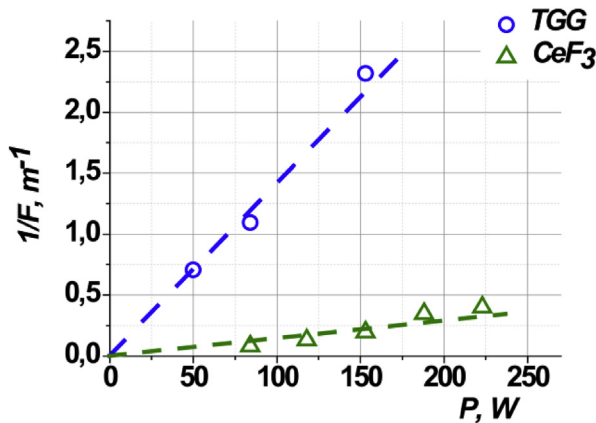


Fig. 6. Thermal lens strength versus laser radiation power for CeF₃ and TGG crystals.

distortions caused by the photo-elastic effect will look qualitatively the same. The quantitative difference is the substitution of the coefficient defined by the components of elastic compliance and thermal expansion tensors similarly to formulas (9) and (6).

Thus, for describing thermal lens in hexagonal and trigonal crystals we can use formula (12) with the substitution of the expression for the constant P :

$$P = \left(\frac{dn}{dT} \right)_{\sigma} + \frac{n_0^3}{4} \frac{\alpha_{11}^T s_{33} - \alpha_{33}^T s_{13}}{s_{11} s_{33} - s_{13}^2} (\pi_{11} + 3\pi_{12}) \quad (14)$$

In this work we also measured the focal distance of the thermal lens arising in the studied CeF₃ crystal sample (having length $L_{\text{CeF}_3} = 7.5$ mm). Measurements were based on the phase-shift interferometry method proposed in Ref. [27]. Optical scheme was the same as in Refs. [28] and [29]. Heating was performed by an Yb-fiber laser ($\lambda = 1075$ nm) with maximum power of 300 W. Beam has Gaussian intensity profile and radius of 0.17 mm. The results of the experiment are presented in Fig. 6 (triangles) for the laser beam.

According to (12), from the $F^{-1}(P_0)$ dependence we can find the magnitude of $\alpha P/\kappa$ as a fitting parameter: $(\alpha P/\kappa)_{\text{CeF}_3} = 8.7 \cdot 10^{-8} \text{ W}^{-1}$. Accuracy of determination of this parameter depends on number of measurements and was about 12% in our case.

The same plot shows for comparison the results of measurements of thermal lens in the TGG crystal having length $L_{\text{TGG}} = 9.5$ mm for the same value of laser beam radius (circles). Taking into account that TGG sample length was 27% larger, from the experimental data and formula (12) we can conclude that the parameter $(\alpha P/\kappa)$ in the CeF₃ crystal is 6.5 times less than in the TGG crystal. Thereby, the thermal lens induced in CeF₃ has a 6.5 lower optical strength for the same laser beam parameters.

Using the results of measurements of the parameter $(\alpha Q/\kappa)$ presented in section 3 we determined the magnitude of the P/Q ratio for the CeF₃ crystal to be 1.53.

5. Discussion of the results

In the present paper we have investigated the thermo-optical and magneto-optical characteristics of the CeF₃ crystal aiming at assessing its potential applications in Faraday isolators for high-power laser systems.

We have shown that the optical anisotropy parameter of the CeF₃ crystal is equal to unity. We have measured the magneto-optical figure of merit of this material and the parameter $\alpha P/\kappa$. According to the experimental data, the magneto-optical figure of merit of the CeF₃ crystal is equal to the magneto-optical figure of

merit of a high-quality TGG crystal and the parameter $\alpha P/\kappa$ is 6.5 times less. It is worthy of notice that we have studied the experimental sample of the medium that was not intended for application in optics. We believe that with the advance of the element production technology, taking into consideration the requirements for optical quality, the reported characteristics will be still better. Thus, from the point of view of thermally induced depolarization, the characteristics of CeF₃ are not inferior to those of TGG, and are superior in terms of thermal lens.

The equality to unity of the optical anisotropy parameter ξ can also be regarded to be the CeF₃ advantage over the TGG crystal whose ξ is 2.25, as in this case there is no need to align the MOE with respect to the polar angle. Moreover, better compensation may be achieved with the use in the FI of a scheme with compensation of thermally induced depolarization by a 67.5-degree rotator [30]. In addition, the optical anisotropy of CeF₃ is small [9], hence, the requirements to MOE alignment along the optical axis during FI assembly will be not too stringent.

The mentioned advantages together with the feasibility of producing large-aperture elements allow us to conclude that the CeF₃ crystal is promising for developing FIs for high-power laser systems.

It is also worth noting that in contrast to TGG, the CeF₃ crystal is transparent to radiation at the wavelength of about 2 μm , which makes it a potential candidate for creating high-power laser systems of this range that has been rapidly developing in the recent years.

Funding

This work was supported by the Russian Foundation for Basic Research [grant number 16-52-50006]; Government of the Russian Federation [grant number 14.B25.31.0024]; and the JSPS KAKENHI [grant numbers 15K13386, 26709072]. This work was also supported by JSPS and RFBR under the Japan - Russia Research Cooperative Program.

References

- [1] E.A. Mironov, O.V. Palashov, Faraday isolator based on TSAG crystal for high power lasers, *Opt. Express* 22 (2014) 23226–23230.
- [2] Ilya L. Snetkov, Ryo Yasuhara, Alexey V. Starobor, Evgeniy A. Mironov, Oleg V. Palashov, Thermo-optical and magneto-optical characteristics of terbium scandium aluminum garnet crystals, *IEEE J. Quantum Electron* 51 (2015) 7000307.
- [3] R. Yasuhara, I. Snetkov, A. Starobor, E. Mironov, O. Palashov, Faraday rotator based on TSAG crystal with <001> orientation, *Opt. Express* 24 (2016) 15486–15493.
- [4] E.A. Mironov, O.V. Palashov, A.V. Voitovich, D.N. Karimov, I.A. Ivanov, Investigation of thermo-optical characteristics of magneto-active crystal Na_{0.37}Tb_{0.63}F_{2.26}, *Opt. Lett.* 40 (2015) 4919–4922.
- [5] D. Zhelezov, A. Starobor, O. Palashov, C. Chen, S. Zhou, High-power Faraday isolators based on TAG ceramics, *Opt. Express* 22 (3) (2014) 2578–2583.
- [6] A. Starobor, D. Zhelezov, O. Palashov, Ch. Chen, Sh. Zhou, R. Yasuhara, Study of the properties and prospects of Ce:TAG and TGG magneto-optical ceramics for optical isolators for lasers with high average power, *Opt. Mater. Express* 4 (2014) 2127–2132.
- [7] E.G. Villora, K. Shimamura, G.R. Plaza, Ultraviolet-visible optical isolators based on CeF₃ Faraday rotator, *J. Appl. Phys.* 117 (2015) 233101.
- [8] P. Molina, V. Vasylyev, E.G. Villora, K. Shimamura, CeF₃ and PrF₃ as UV-visible Faraday rotators, *Opt. Express* 19 (2011) 11786–11791.
- [9] V. Vasylyev, E.G. Villora, M. Nakamura, Y. Sugahara, K. Shimamura, UV-visible Faraday rotators based on rare-earth fluoride single crystals: LiREF₄ (RE = Tb, Dy, Ho, Er and Yb), PrF₃ and CeF₃, *Opt. Express* 20 (2012) 14460.
- [10] C. Pedrini, A.N. Belsky, B. Moine, D. Bouttet, Fluorescence processes and scintillation of CeF₃ crystals excited UV and X-ray synchrotron radiation, *Acta Phys. Pol. A* 84 (1993) 953–957.
- [11] P. Belli, R. Bernabei, R. Cerulli, C.J. Dai, F.A. Danevich, A. Incicchitti, V.V. Kobaychev, O.A. Ponkratenko, D. Proserpi, V.I. Tretyak, Yu.G. Zdesenko, Performances of a CeF₃ crystal scintillator and its application to the search for rare processes, *Nucl. Instrum. Meth. A* 498 (2003) 352–361.
- [12] E.A. Mironov, D.S. Zhelezov, A.V. Starobor, A.V. Voitovich, O.V. Palashov, A.M. Bulkanov, A.G. Demidenko, Large-aperture Faraday isolator based on a

- terbium gallium garnet crystal, *Opt. Lett.* 22 (2015) 2578–2583.
- [13] D.S. Zhelezov, A.V. Starobor, O.V. Palashov, Characterization of the terbium-doped calcium fluoride single crystal, *Opt. Mater.* 46 (2015) 526–529.
- [14] H. Yoshida, K. Tsubakimoto, Y. Fujimoto, K. Mikami, H. Fujita, N. Miyanaga, H. Nozawa, H. Yagi, T. Yanagitani, Y. Nagata, H. Kinoshita, Optical properties and Faraday effect of ceramic terbium gallium garnet for a room temperature Faraday rotator, *Opt. Express* 19 (2011) 15181–15187.
- [15] A.K. Cheetham, B.E.F. Fender, A powder neutron diffraction study of lanthanum and cerium trifluorides, *Acta Cryst. B* 32 (1976) 94–97.
- [16] Ikuo Nishida, Kazuyoshi Tatsumi, Shunsuke Muto, Local electronic and atomic structure of Ce³⁺-Containing fluoride/oxide determined by TEM-EELS and first-principles calculations, *Mater. Trans.* 50 (2009) 952–958.
- [17] M.L. Afanasiev, S.P. Habuda, A.G. Lundin, The symmetry and basic structures of LaF₃, CeF₃, PrF₃ and NdF₃, *Acta Cryst. B* 28 (1972) 2903–2905.
- [18] S. Hart, The elastic constants of cerium fluoride, *Phys. Status Solidi A* 17 (1973) K107.
- [19] J.F. Nye, *Physical Properties of Crystals*, Oxford University Press, London, 1964.
- [20] E.A. Khazanov, O.V. Kulagin, S. Yoshida, D.B. Tanner, D.H. Reitze, Investigation of self-induced depolarization of laser radiation in terbium gallium garnet, *IEEE J. Quantum Electron* 35 (1999) 1116–1122.
- [21] E.A. Khazanov, Faraday Isolators for high average power lasers, in: M. Grishin (Ed.), *Advances in Solid State Lasers Development and Applications*, INTECH, 2010, pp. 45–72.
- [22] Yu.I. Sirotnin, Thermal stresses arising during heating and cooling of monocrystals, *Crystallography* 1 (1956) 708–717 (in Russian).
- [23] D. Brückus, A.S. Dement'ev, On the use of photoelastic effect and plane strain or plane stress approximation of thermal lensing, *Lithuanian J. Phys.* 56 (2016) 9–20.
- [24] Ilya Snetkov, Anton Vyatkin, Oleg Palashov, Efim Khazanov, Drastic reduction of thermally induced depolarization in CaF₂ crystals with [111] orientation, *Opt. Express* 20 (2012) 13357–13367.
- [25] E.A. Mironov, A.G. Vyatkin, A.V. Starobor, O.V. Palashov, Thermo-optical characteristics of DKDP crystal, *Las. Phys. Lett.* 14 (2017) 035801.
- [26] A.K. Potemkin, E.A. Khazanov, Calculation of the laser-beam M2 factor by the method of moments, *Quantum Electron.* 35 (2005) 1042–1044.
- [27] I.E. Kozhevnikov, D.E. Silin, Optical interference methods of subwavelength-resolution imaging, *Radiophys. Quantum Electron* 52 (2009) 67–77.
- [28] I.L. Snetkov, et al., Study of the thermo-optical constants of Yb doped Y2O3, Lu2O3 and Sc2O3 ceramic materials, *Opt. Exp.* 21 (2013) 21254–21263.
- [29] A. Starobor, O. Palashov, Thermal effects in the DKDP Pockels cells in the 215–300 K temperature range, *Appl. Opt.* 55 (2016) 7365–7370.
- [30] E.A. Khazanov, Compensation of thermally induced polarization distortions in Faraday isolators, *Quantum Electron.* 29 (1999) 59–64.